# Vectorial solitary waves in optical media with a quadratic nonlinearity

U. Peschel, C. Etrich, and F. Lederer
*Institut für Festkörpertheorie und Theoretische Optik, Friedrich-Schiller-Universität, Jena, Max-Wien Platz 1, D-07743, Jena, Germany*

B. A. Malomed
*Department of Applied Mathematics, School of Mathematical Sciences, Tel Aviv University, Tel Aviv 69978, Israel*
(Received 3 July 1996)

We search for self-trapped beams due to the vectorial interaction of two orthogonally polarized components of a fundamental harmonic and a single component of the second harmonic in a quadratically nonlinear medium. The basic set of equations for both the temporal and the spatial case is derived. The resulting two-parameter family of solitary waves is investigated by means of a variational approximation and by direct numerical methods. Several limiting cases and differences to the scalar interaction in quadratic media are discussed. The propagation of stable solitary waves and mutual collisions are simulated and the decay of unstable solitary waves is demonstrated. We predict an internal boundary in the soliton parameter space which separates stable and unstable domains. [S1063-651X(97)06806-2]

PACS number(s): 42.65.Tg, 42.65.Ky

## I. INTRODUCTION

For many decades solitons have attracted a great deal of interest because of their robust, particlelike behavior. They may be regarded as fundamental excitations of various nonlinear systems in biology, chemistry, or physics. In particular, the resonant as well as nonresonant interaction of light with matter was shown to create an ideal environment for solitons to exist. Self-induced transparency solitons travel without any losses through an ensemble of resonant two-level systems and collide without losing their stability [1]. Instantaneous cubic (Kerr) nonlinearities which are based on nonresonant effects may prevent the diffraction-induced spreading of beams or dispersion-induced broadening of pulses. The evolution of the corresponding spatial and temporal envelope solitons may be described by the nonlinear Schrödinger equation. Spatial solitons were found to exist in many transparent materials like fused silica [2], semiconductors [3], and liquids [4]. Particular emphasis was paid to the investigation of the propagation of temporal solitons in fibers because of their potential use as a fundamental bits in high bit-rate, long-haul signal-transmission systems [5,6].

In recent years a renewed interest emerged regarding quadratic nonlinearities arising in noncentrosymmetric materials like potassium titanyl phosphate (KTP), lithium niobate ($LiNbO_3$), and poled polymers. Earlier investigations were primarily concentrated on the efficient frequency conversion of the light field. Now two new issues are of interest. First as an alternative for using cubic nonlinearities in all-optical switching schemes it was proposed to exploit phase and amplitude modulation of the fundamental harmonic generated by consecutive up and down conversion.

Indeed, large nonlinearly induced phase shifts of the fundamental harmonic (FH) were observed in KTP crystals [7], in $LiNbO_3$ channel waveguides [8], and in phase matched KTP waveguides [9,10]. In this context it may be anticipated that novel all-optical operations can be implemented and that the required switching power can be reduced. Recently the validity of this scheme was demonstrated experimentally. Large amplitude modulations of the FH were induced by varying the phase of the second harmonic (SH) [11]. Even basic photonic components such as nonlinear directional couplers [12] and Mach-Zehnder interferometers [13] based on $LiNbO_3$ channel waveguides were successfully operated.

Secondly it was found that this phase modulation may balance the dispersion- (diffraction-) induced pulse broadening (beam spreading). As a consequence mutually trapped solitary waves (SW) may be formed consisting of the fundamental and second harmonics [14–28]. A one-parametric family of solutions was numerically determined [20] with the exception of one element which is known analytically [14]. Both stable and unstable SWs were found and the corresponding parameter ranges were identified [22,23]. Recently, the collision of these SWs has been studied [24,25]. As could be anticipated for a nonintegrable system, it was found that the colliding SWs fuse for sufficiently small relative velocities.

As a matter of fact, the existence of spatial bright SWs was experimentally demonstrated in planar $LiNbO_3$ waveguides [26]. In comparison to cubic nonlinearities the interaction of two waves evokes novel effects. A representative example is the stable propagation of two-dimensional self-guided beams in a KTP-bulk crystal [27,28] which contrasts the catastrophic self-focusing in a cubic nonlinearity. Until now the interest was almost exclusively focused on the situation where one FH and SH component are involved. Obviously, the degrees of freedom of the dynamical system will increase if the number of interacting waves increases. This can be achieved by leaving the degenerated case and studying the three-wave parametric interaction [29] or by exploiting the so-called type-II phase matching (vectorial interaction) [30]. In the latter case two orthogonally polarized FH components create a single SH field which is then down converted to both FHs.

This type of interaction has already attracted a great deal of interest in situations where dispersion and diffraction can be neglected [31–38]. The power imbalance between the FHs represents an additional control parameter. It offers an-

 

other opportunity to tune the nonlinear interaction and can be used to create novel effects which are based on amplitude and phase modulation. In particular, the nonlinearly induced phase shift of every FH depends on this new degree of freedom very sensitively [34,35]. A number of experiments were devoted to this subject. Nonlinearly induced polarization rotation was observed [37,38] and a transistorlike switching behavior could be obtained [36].

The aim of the present work is to include diffraction and dispersion into the study of the vectorial interaction and to search for solitary-wave solutions. We restrict ourselves to the one-dimensional case which is relevant for self-guided beams in planar waveguides or for pulses propagating in channel waveguides or fibers. The basic set of normalized equations likewise describes the situation of the nondegenerated parametric interaction. This case was studied in a recent paper [39]. Although it has been shown that the set of normalized equations exhibits solitary-wave solutions, which were termed ''three-wave bright spatial solitons,'' the ''physical'' equations used in this work do not describe at all the propagation of light beams in a planar waveguide as claimed. Nevertheless the conclusions drawn from the formal solutions are interesting and show that a two-parametric family of stationary localized solutions exists. Evidently, SWs known from the scalar interaction appear in the limiting case of balanced excitation of both FHs. Moreover, it was pointed out that in some particular cases one of the three fields can be expressed by the two remaining ones. This holds not only for the Schrödinger limit as it does for the scalar interaction and large phase mismatch but also for an extreme imbalance of the FH waves. But even in this case an analytical solution exists only if both remaining fields are equal. Hence in the present paper the main emphasis is on the analytical description of the vectorial SWs, and on effects which are due to the vectorial nature of the interaction, on the stability, and on the collision behavior.

The paper is organized as follows. In Sec. II we derive the basic set of equations which describe both the propagation of short pulses and narrow beams in quadratically nonlinear waveguides. We determine the respective integrals of motion. In Sec. III we proceed with the variational approach which gives a fully analytical description of the solitary-wave solution. We compare our analytical results with those obtained by a direct numerical integration and study the dynamical behavior of the stationary solutions in Sec. IV. Furthermore, we propagate some of the field profiles obtained and discuss the stability and the collision behavior of the solutions.

## II. THE MODEL

In this section we derive the basic equations which apply to both pulse and beam propagation in quadratically nonlinear waveguides. We start from the most general model describing the vectorial interaction between the slowly varying envelopes of the two FHs $\tilde{E}_1$, $\tilde{E}_2$ and the SH $\tilde{E}_3$,

$$\left[ i \frac{\partial}{\partial z} + i a_1 \frac{\partial}{\partial \tilde{x}} + b_1 \frac{\partial^2}{\partial \tilde{x}^2} \right] \tilde{E}_1 + \chi_1 \tilde{E}_2^* \tilde{E}_3 = 0, \tag{1}$$

$$\left[ i \frac{\partial}{\partial z} + i a_2 \frac{\partial}{\partial \tilde{x}} + b_2 \frac{\partial^2}{\partial \tilde{x}^2} \right] \tilde{E}_2 + \chi_2 \tilde{E}_1^* \tilde{E}_3 = 0, \tag{2}$$

$$\left[ i \frac{\partial}{\partial z} + i a_3 \frac{\partial}{\partial \tilde{x}} + b_3 \frac{\partial^2}{\partial \tilde{x}^2} - \tilde{q} \right] \tilde{E}_3 + \chi_3 \tilde{E}_1 \tilde{E}_2 = 0, \tag{3}$$

where $z$ denotes the direction of propagation and $\tilde{x}$ the transverse coordinate of a beam in a planar waveguide or the time of a pulse in a channel waveguide. The coefficients $a_n$ ($n=1,2,3$) and $b_n$ are uniquely determined by the $z$ component $k_z^{(n)}$ of the propagation vector $\vec{k}^n$ of each wave. In the spatial case they represent the so-called beam walk off $a_n = \partial k_z^{(n)} / \partial k_x^{(n)}$ and the diffraction coefficients in the planar waveguide $b_n = 1/(2k_z^{(n)})$, whereas in the temporal case they stand for the inverse group velocity $a_n = \partial k_z^{(n)} / \partial \omega$ and the group-velocity dispersion in a channel waveguide $b_n = \partial^2 k_z^{(n)} / \partial \omega^2$. $\tilde{q} = k_z^{(1)} + k_x^{(2)} - k_z^{(3)}$ is the wave vector mismatch and $\chi_n$ are the effective second-order nonlinear coefficients averaged with the mode profiles (see [35]). Now we proceed as in the scalar case. First we change to a moving reference frame where all fields are at rest, thus eliminating the first derivatives with respect to $\tilde{x}$. This can be achieved by appropriate shifts of the center frequency of the waves involved [20]. Next we introduce the propagation constants of the solitary waves $\kappa_{1/2}$. These transformations are

$$\tilde{E}_{1/2}(\tilde{x},z) = E_{1/2}(x,z) \exp(i \kappa_{1/2} z - i \omega_{1/2} x),$$

$$\tilde{E}_3(\tilde{x},z) = E_3(x,z) \exp(i[\kappa_1 + \kappa_2] z - i[\omega_1 + \omega_2] x),$$

$$x = \tilde{x} - \frac{z}{v}. \tag{4}$$

Note that the existence of solitary-wave solutions $E_{1/2}(x,z) = E_{1/2}(x)$ implies nonlinearly induced phase matching [39]. The frequency shift and the velocity of the reference frame are given by

$$\omega_{1/2} = \frac{b_{2/1}(a_3 - a_{1/2}) + b_3(a_{1/2} - a_{2/1})}{2[(b_1 + b_2) b_3 - b_1 b_2]},$$

$$\frac{1}{v} = \frac{a_1 b_2 b_3 - a_3 b_1 b_2 + a_2 b_1 b_3}{(b_1 + b_2) b_3 - b_1 b_2}. \tag{5}$$

The rescaled set of equations is

$$\left[ i \frac{\partial}{\partial z} + b_1 \frac{\partial^2}{\partial x^2} - \kappa_1 \right] E_1 + \chi_1 E_2^* E_3 = 0, \tag{6}$$

$$\left[ i \frac{\partial}{\partial z} + b_2 \frac{\partial^2}{\partial x^2} - \kappa_2 \right] E_2 + \chi_2 E_1^* E_3 = 0, \tag{7}$$

$$\left[ i \frac{\partial}{\partial z} + b_3 \frac{\partial^2}{\partial x^2} - (q + \kappa_1 + \kappa_2) \right] E_3 + \chi_3 E_1 E_2 = 0, \tag{8}$$

where the mismatch $q$ is now defined at the new carrier frequencies:

$$q = \tilde{q} - b_1 \omega_1^2 - b_2 \omega_2^2 + b_3 (\omega_1 + \omega_2)^2. \tag{9}$$

Regarding the transformation (4) some additional remarks should be made. As far as planar waveguides without walk off are considered, Eqs. (6)–(8) can be used directly. If the walk-off terms are present (first derivatives with respect to $\tilde{x}$) the above transformation can be applied formally if the denominator in Eq. (5), $(b_1+b_2)b_3-b_1b_2$, differs from zero. Unfortunately, it is very close to zero if the coefficients $b_n$ describe diffraction rather than dispersion. Hence we will not address the case of spatial walk off in this paper. If these coefficients describe group-velocity dispersion (temporal case) the transformation may always be applied provided that the paraxial approximation is valid for the shifted carrier frequency. We note that these frequency shifts $\omega_1$ and $\omega_2$ may differ. Then the resulting equations hold for slowly varying envelopes of two FHs with different carrier frequencies.

We are interested in bright SWs which exist for $b_{1/2}\kappa_{1/2}>0$ and $b_3(q+\kappa_1+\kappa_2)>0$ only. Here we restrict to $b_n>0$, which corresponds to the spatial case or to anomalous dispersion if pulses are concerned. Changing to the case $b_n<0$ corresponds to a simple phase transformation. A final transformation removes the dependence on the actual magnitude of $b_n$ [20]:

$$\left[i\delta\frac{\partial}{\partial Z}+\frac{1}{2}\frac{\partial^2}{\partial X^2}-\beta\right]A_1+A_2^*A_3=0, \tag{10}$$

$$\left[\frac{i}{\delta}\frac{\partial}{\partial Z}+\frac{1}{2}\frac{\partial^2}{\partial X^2}-\frac{1}{\beta}\right]A_2+A_1^*A_3=0, \tag{11}$$

$$\left[i\sigma\frac{\partial}{\partial Z}+\frac{1}{2}\frac{\partial^2}{\partial X^2}-\alpha\right]A_3+A_1A_2=0, \tag{12}$$

with

$$X=\frac{x}{X_0},\quad Z=\frac{z}{Z_0},\quad A_n=\frac{E_n}{E_n^0},$$

$$X_0=\left(\frac{4b_1b_2}{\kappa_1\kappa_2}\right)^{1/4},\quad Z_0=(\kappa_1\kappa_2)^{-1/2},$$

$$E_{1/2}^0=\left(\frac{\kappa_1\kappa_2 b_3}{b_{1/2}|\chi_{2/1}\chi_3|}\right)^{1/2},$$

$$E_3^0=\left(\frac{\kappa_1\kappa_2}{|\chi_1\chi_2|}\right)^{1/2}.$$

The dispersion-diffraction coefficients $b_n$ enter only via the terms $\delta$ and $\sigma$ as

$$\delta=\left(\frac{b_2}{b_1}\right)^{1/2},\quad \sigma=\left(\frac{b_1b_2}{b_3^2}\right)^{1/2}.$$

The stationary solutions to Eqs. (10)–(12), i.e., the solitary waves, are completely determined by the parameters

$$\alpha=\left(\frac{b_1b_2}{b_3^2\kappa_1\kappa_2}\right)^{1/2}(\kappa_1+\kappa_2+q)\quad\text{and}\quad\beta=\left(\frac{b_2\kappa_1}{b_1\kappa_2}\right)^{1/2}$$

thus forming a two-parameter family of solutions. $\alpha$ and $\beta$ have to be positive. In particular $\beta=1$ corresponds to the scalar case. The solutions are symmetric with respect to an interchange of pairs $(\beta,A_1)$ and $(1/\beta,A_2)$ which holds also for nonstationary solutions if $\delta=1$. Thus we may restrict our analysis to the interval $0<\beta\leqslant 1$. It is worth mentioning that all SWs with $\alpha<\sigma(\beta/\delta+\delta/\beta)$ correspond to negative mismatch ($q<0$, area left of the dotted line in Fig. 2). Two trivial phase symmetries can be found in the system:

$$A_1\exp(i\phi_1),\quad A_2\exp(i\phi_2),\quad A_3\exp(i\phi_1+i\phi_2). \tag{13}$$

The two FHs are determined up to two constant phase factors. The general behavior of a single SW is not affected by the mutual phase relation between both FH waves. Hence the FH waves of a SW may vary between linear ($\phi_1=\phi_2+m\pi$, $m=0,1,2,\ldots$) and circular ($\phi_1=\phi_2+m\pi/2$, $m=1,3,5\ldots$) polarization without affecting the field structure. In contrast to the scalar interaction the additional degree of freedom with respect to the phases of the FH waves generates a new conservation law. In analogy to the Manley-Rowe relations [29] in the continuous wave case three conserved quantities can be identified, viz., the total energy

$$Q\equiv\int_{-\infty}^{+\infty}\left(\delta|A_1|^2+\frac{1}{\delta}|A_2|^2+2\sigma|A_3|^2\right)dx, \tag{14}$$

the energy imbalance between both FH components,

$$R\equiv\int_{-\infty}^{+\infty}\left(\delta|A_1|^2-\frac{1}{\delta}|A_2|^2\right)dx, \tag{15}$$

and the Hamiltonian

$$H\equiv\int_{-\infty}^{+\infty}\left(\frac{1}{2}\left|\frac{\partial A_1}{\partial x}\right|^2+\frac{1}{2}\left|\frac{\partial A_2}{\partial x}\right|^2+\frac{1}{2}\left|\frac{\partial A_3}{\partial x}\right|^2-q'\sigma|A_3|^2-A_1^*A_2^*B-A_1A_2B^*\right)dx. \tag{16}$$

In particular, the conservation of the energy imbalance describes the permanent vectorial character of the interaction. Furthermore, the Hamiltonian depends merely on the scaled mismatch $q'=qZ_0$ which can be expressed by the parameters $\alpha$ and $\beta$:

$$q'=\frac{\alpha}{\sigma}-\left(\frac{\beta}{\delta}+\frac{\delta}{\beta}\right). \tag{17}$$

For completeness we give the fourth conserved quantity, the momentum $P$,

$$P=i\int_{-\infty}^{+\infty}\left[\delta\left(A_1^*\frac{\partial A_1}{\partial x}-A_1\frac{\partial A_1^*}{\partial x}\right)+\frac{1}{\delta}\left(A_2^*\frac{\partial A_2}{\partial x}-A_2\frac{\partial A_2^*}{\partial x}\right)+\sigma\left(A_3^*\frac{\partial A_3}{\partial x}-A_3\frac{\partial A_3^*}{\partial x}\right)\right]dx, \tag{18}$$

which vanishes for all resting or real-valued solutions.

The system of Eqs. (10)–(12) is not integrable. The only exact, analytical solution for $\alpha=\beta=1$ requires equal $\mathrm{sech}^2$

envelopes for all three waves. It is the trivial extension of the scalar solution [14] and is given in [39]. Note that due to the phase symmetry given in Eq. (13) this solution may have different phases in both FHs and thus may differ from the scalar case substantially.

Since the Schrödinger limit was already discussed in [39] we search for stationary solutions of Eqs. (10)–(12) for arbitrary $\alpha$ and $\beta$. Because the stationary SW solutions are real valued in the scalar interaction we restrict ourselves to this case too. These solutions correspond to the motion of a particle in the three-dimensional potential [39]

$$V_{\mathrm{eff}}=A_1A_2A_3-\frac{\beta}{2}A_1^2-\frac{1}{2\beta}A_2^2-\frac{\alpha}{2}A_3^2, \tag{19}$$

which is zero at the origin. Because the field of a bright SW has to vanish if $x\to\pm\infty$ the motion starts and terminates at the origin. The turning point is determined by $V_{\mathrm{eff}}=0$ and yields the peak amplitudes of the waves:

$$\beta(A_1^{\max})^2+\frac{1}{\beta}(A_2^{\max})^2+\alpha(A_3^{\max})^2=2A_1^{\max}A_2^{\max}A_3^{\max}. \tag{20}$$

Obviously none of the amplitudes can vanish. Moreover they are subject to the constraints

$$A_1^{\max}>\left(\frac{\alpha}{\beta}\right)^{1/2},\quad A_2^{\max}>\sqrt{\alpha\beta},\quad A_3^{\max}>1. \tag{21}$$

In particular, the maximum intensity of the FH,

$$(A_1^{\max})^2+(A_2^{\max})^2>\alpha\left(\beta+\frac{1}{\beta}\right)>2\alpha, \tag{22}$$

diverges if $\alpha$, $\beta$, or $1/\beta$ approach infinity.

### III. THE VARIATIONAL APPROXIMATION

In this section we will employ the variational approximation in order to achieve a family of solitary-wave solutions to Eqs. (10)–(12) in an approximate analytical form.

The ordinary differential equations describing stationary real-valued solutions of Eqs. (10)–(12) can be derived from the Lagrangian

$$L=\int_{-\infty}^{+\infty}\left[\frac{1}{4}(A_1')^2+\frac{1}{4}(A_2')^2+\frac{1}{4}(A_3')^2+\frac{\beta}{2}A_1^2+\frac{1}{2\beta}A_2^2+\frac{\alpha}{2}A_3^2-A_1A_2A_3\right]dx, \tag{23}$$

where the primes denote the derivative with respect to $x$.

Now we proceed as usual, choosing as trial function for the fields a simple Gaussian ansatz

$$A_n=u_n\exp(-\tfrac{1}{2}\rho_n x^2), \tag{24}$$

with $u_n$ and $\rho_n$ real. Substituting this trial function into the Lagrangian and integrating we arrive at the following effective Lagrangian for the free parameters $u_n$ and $\rho_n$:

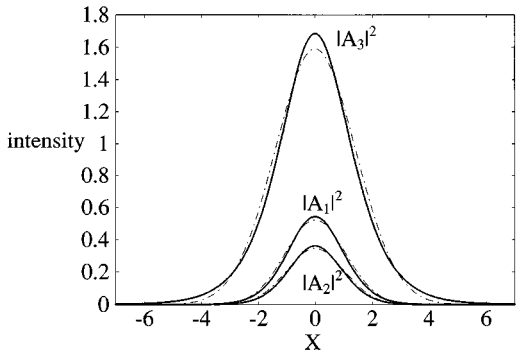


FIG. 1. Field structures of the SWs (solid line) in comparison with the results obtained from the Lagrangian approach (dashed-dotted line). Parameters: $\alpha=0.156$, $\beta=0.778$.

$$\frac{L}{\sqrt{\pi}}=\frac{1}{8}u_1^2\sqrt{\rho_1}+\frac{1}{8}u_2^2\sqrt{\rho_2}+\frac{1}{8}u_3^2\sqrt{\rho_3}+\frac{\beta}{2}\rho_1^{-1/2}u_1^2+\frac{1}{2\beta}\rho_2^{-1/2}u_2^2+\frac{\alpha}{2}\gamma^{-1/2}u_3^2-\sqrt{2}(\rho_1+\rho_2+\rho_3)^{-1/2}u_1u_2u_3. \tag{25}$$

We are now looking for extrema of $L$. The conditions $\partial L/\partial u_n=0$ yield the amplitudes $u_n$ in terms of the inverse widths $\rho_n$:

$$u_1^2=\frac{\rho_1+\rho_2+\rho_3}{2\sqrt{\rho_2\rho_3}}\left(\frac{1}{\beta}+\frac{1}{4}\rho_2\right)\left(\alpha+\frac{1}{4}\rho_3\right), \tag{26}$$

$$u_2^2=\frac{\rho_1+\rho_2+\rho_3}{2\sqrt{\rho_1\rho_3}}\left(\beta+\frac{1}{4}\rho_1\right)\left(\alpha+\frac{1}{4}\rho_3\right), \tag{27}$$

$$u_3^2=\frac{\rho_1+\rho_2+\rho_3}{2\sqrt{\rho_1\rho_2}}\left(\beta+\frac{1}{4}\rho_1\right)\left(\frac{1}{\beta}+\frac{1}{4}\rho_2\right). \tag{28}$$

If we apply the conditions $\partial L/\partial\rho_n=0$ and eliminate the amplitudes $u_n$ by means of Eqs. (26)–(28), the soliton parameters $\alpha$ and $\beta$ as well as the inverse width of the SH beam $\rho_3$ can be expressed in terms of $\rho_1$ and $\rho_2$.

$$\rho_3=\frac{1}{16-\rho_1\rho_2}[\sqrt{(\rho_1\rho_2+16)^2(\rho_1-\rho_2)^2+256\rho_1^2\rho_2^2}+2\rho_1\rho_2(\rho_1+\rho_2)], \tag{29}$$

$$\alpha=\frac{\rho_3(\rho_1+\rho_2+3\rho_3)}{4(\rho_1+\rho_2-\rho_3)}, \tag{30}$$

$$\beta=\frac{\rho_1(3\rho_1+\rho_2+\rho_3)}{4(\rho_2-\rho_1+\rho_3)}. \tag{31}$$

For fixed parameters $\alpha$ and $\beta$ the width parameters $\rho_n$ can be determined numerically by inverting Eqs. (29)–(31). We found the width parameters to be uniquely determined by the parameters $\alpha$ and $\beta$. The amplitudes $u_n$ can be calculated by means of Eqs. (26)–(28). One example of a SW which is determined in this way is displayed in Fig. 1. Although the

parameters $\alpha$ and $\beta$ have rather extreme values the Gaussian matches the exact field structure quite well.

A second and maybe more convenient way is to regard $\rho_1$ and $\rho_2$ as a new set of independent parameters. With respect to this alternative notation SW solutions exist for $\rho_1\rho_2<16$ [see the denominator of Eq. (29)] and are obviously symmetric with respect to an interchange of $\rho_1$ and $\rho_2$. All three width parameters $\rho_i$ obey the inequality of a triangle $\rho_i+\rho_j>\rho_k$. All the amplitudes depend on the width parameters explicitly [see Eqs. (26)–(28)] and hence also the conserved quantities [see Eqs. (14)–(16)] can be expressed analytically.

The analytical expressions derived above provide us with a powerful tool to investigate the behavior of the SWs in some limiting cases. For large $\alpha$ and subsequently for positive mismatch [see Eq. (17)] the width parameters of both FH beams are restricted to a hyperbola defined by $(2\rho_1+\rho_2)(2\rho_2+\rho_1)=16$, while for the inverse width of the SH beam we have $\rho_3=\rho_1+\rho_2$. The squared amplitudes of the SH beam $u_3^2$ remain finite while $u_1^2$ and $u_2^2\to\infty$ [see inequality (21)]. The energy of the whole system is stored in the FH waves and diverges with increasing amplitudes or proportionally to $\alpha$. The relation between energy imbalance and total energy [see Eqs. (14) and (15)] is

$$\frac{R}{Q}=\frac{\delta^2\rho_2^2-\rho_1^2}{\delta^2\rho_2^2+\rho_1^2} \tag{32}$$

and varies between $-1$ and $+1$. In agreement with the findings in [39] the peculiarities of the vectorial interaction are maintained and the system does not converge to the scalar case.

For $\alpha\to 0$ a second interesting limiting case is obtained. It corresponds to a negative mismatch. It follows from Eqs. (29)–(31) that all width parameters $\rho_i$ vanish too. Hence the beams become infinitely broad. A more detailed analysis reveals that the width parameter $\rho_3$ of the SH beam tends to zero proportionally to $\alpha$, where those of the FH beams ($\rho_{1/2}$) diminish proportionally to $\sqrt{\alpha}$ only. Thus more and more of the energy is carried by the SH. The relation between total energy and energy imbalance is for small $\alpha$.

$$\frac{R}{Q}=\frac{2(\delta^2-\beta^2)}{\beta\delta\sigma}\,\alpha. \tag{33}$$

Hence all the field distributions converge to those known from the scalar case.

A third limiting case occurs for diverging wave vector imbalance if $\beta$ approaches either zero or infinity. As already mentioned, this case is closely related to the situation where $\alpha\to\infty$ [39]. It suffices to deal with the case of vanishing $\beta$. This limiting case corresponds to a negative mismatch [see Eq. (17)]. All width parameters tend to zero. Whereas $\rho_2$ and $\rho_3$ decrease proportionally to $\sqrt{\beta}$, $\rho_1$ falls more rapidly like $\beta$ itself. Consequently the first FH wave contains all the energy. It grows to infinity proportionally to $\beta^{-3/2}$. For the ratio between energy imbalance and total energy we obtain $R/Q=+1$.

It might be interesting to translate the analytical results obtaining to the experimental situation. We demonstrate this by means of the SW displayed in Fig. 1. All quantities are determined for a spatial SW which propagates in an ion-implanted planar waveguide (thickness about 4 $\mu$m) on top of a KTP crystal. We assume a FH wavelength of $\lambda=1.064$ $\mu$m where phase matching is achieved by coupling of two orthogonal FH modes (nonlinear coefficient: $d_{\rm eff}=3.1$ pm/V, for more details concerning the derivation see, e.g., [35]). The diffraction coefficients are given by $b_1=b_2=\lambda/4/\pi$ and $b_3=b_2/2$. It is evident that the results critically depend on the mismatch which can be tuned within a certain range. For the SW displayed in Fig. 1 a negative mismatch is required. Its optimum value results from a trade-off between minimal power requirements and an acceptable beam width. Note that all intensities scale with the squared mismatch and the beam width decreases with the square root of the mismatch. Consequently the total energy of the SW grows as $|q|^{3/2}$. Here we assume a mismatch of $q=-10$/cm which is a typical value experimentally achieved [33]. We use the approximate analytical solutions to determine the relevant parameters required to perform an experiment. We fix both width parameters $\rho_1=0.445$ and $\rho_2=0.491$ of the FH wave and obtain from Eqs. (29)–(31) $\rho_3=0.253$, $\alpha=0.156$, and $\beta=0.778$. The amplitudes are determined by using Eqs. (26)–(28) as $u_1^2=0.523$, $u_2^2=0.346$, and $u_3^2=1.59$. Integrating the trial functions we obtain the normalized energy of the SW $Q=7.8$ as well as the relative imbalance $R/Q=0.0637$. Now we undo the normalization and determine the corresponding unscaled wave numbers

$$\kappa_1=\frac{qb_1\beta^2}{b_3\alpha\beta-b_2-b_1\beta^2},\quad \kappa_2=\frac{qb_2}{b_3\alpha\beta-b_2-b_1\beta^2} \tag{34}$$

to be $\kappa_1=3.92$/cm and $\kappa_2=6.47$/cm. It is now straightforward to calculate the respective power and the beam width. The total power carried by the SW is 2.34 kW, where the width of the beam is mainly determined by the SH component and amounts to 55.6 $\mu$m.

## IV. NUMERICAL RESULTS

The SW solutions of Eqs. (10)–(12) for different values of $\alpha$ and $\beta$ were determined using a Newton iteration scheme. We are interested in single hump solutions only. A typical field structure is displayed in Fig. 1 together with the corresponding Gaussian obtained from the Lagrangian approach. Obviously the Gaussian fits quite well to the exact fields. Furthermore, we have calculated both the total energy $Q$ and the relative energy imbalance $R/Q$ in a wide parameter range (see Fig. 2). The upper boundary of both figures corresponds to the scalar case ($\beta=1$). Again the agreement between the Lagrangian approach and the exact solution is very good and the predictions with respect to the different limiting cases are verified. In general the total energy increases if $\beta$ deviates from 1. It can be clearly recognized from Fig. 2(a) that the total energy diverges if one of the parameters $\alpha$ or $\beta$ approaches zero or infinity. Furthermore, the energy imbalance vanishes together with $\alpha$ and we can expect the system to converge to the scalar case [see Fig. 2(b)]. Note that no significant changes occur if the mismatch changes its sign.

The next step is to solve the system of partial differential equations (10)–(12) numerically with any stationary solution

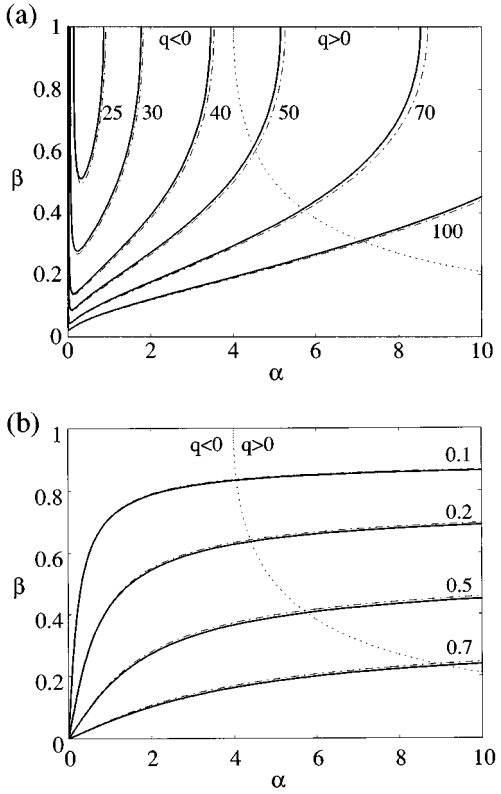


FIG. 2. Contour plots of the energy $Q$ (a) and the relative energy imbalance $Q/R$ (b) of spatial vectorial solitons vs the soliton parameters $\alpha$ and $\beta$ ($\delta=1$, $\sigma=2$). Solid line: numerical calculation; dashed-dotted line: variational approach; dotted line: zero mismatch.

as the initial condition. This is done by using a standard beam propagation method (BPM). A simple collision experiment reveals that two SWs fuse if their interaction angle or their relative velocity is less than a critical value (see Fig. 3). Hence we may draw the conclusion that, similarly to the scalar case [24], the solutions under consideration are solitary waves rather than solitons.

In analogy to the scalar case both stable [Fig. 4(a)] and unstable solutions exist [Fig. 4(b)]. Unstable solutions need not decay but can instead propagate over large distances where they are subject to persistent oscillations [22]. This behavior is maintained in the vectorial case as can be seen in Fig. 4(b). It can be recognized from Fig. 4 that small changes in the imbalance $\beta$ may essentially affect the stability behavior, i.e., an increasing imbalance and thus a more pronounced vectorial interaction seems to lead to an effective stabilization of the SWs. Even for parameters $\alpha$ where scalar SWs become unstable [22] vectorial SWs propagate stably.

To clarify this issue we make use of a criterion frequently employed in probing the soliton stability [40]. One has to investigate, for example, the Hamiltonian as a function of the conserved quantities left. If the resulting function is multivalued only one branch is stable. A transition from one branch to another results in a change of the stability. In the scalar case with negative mismatch the Hamiltonian is a double-valued function of the energy. The stability changes at a minimum of the energy of the SW. In the case of the vectorial interaction both the energy and the energy imbalance have to be considered. In performing this analysis it

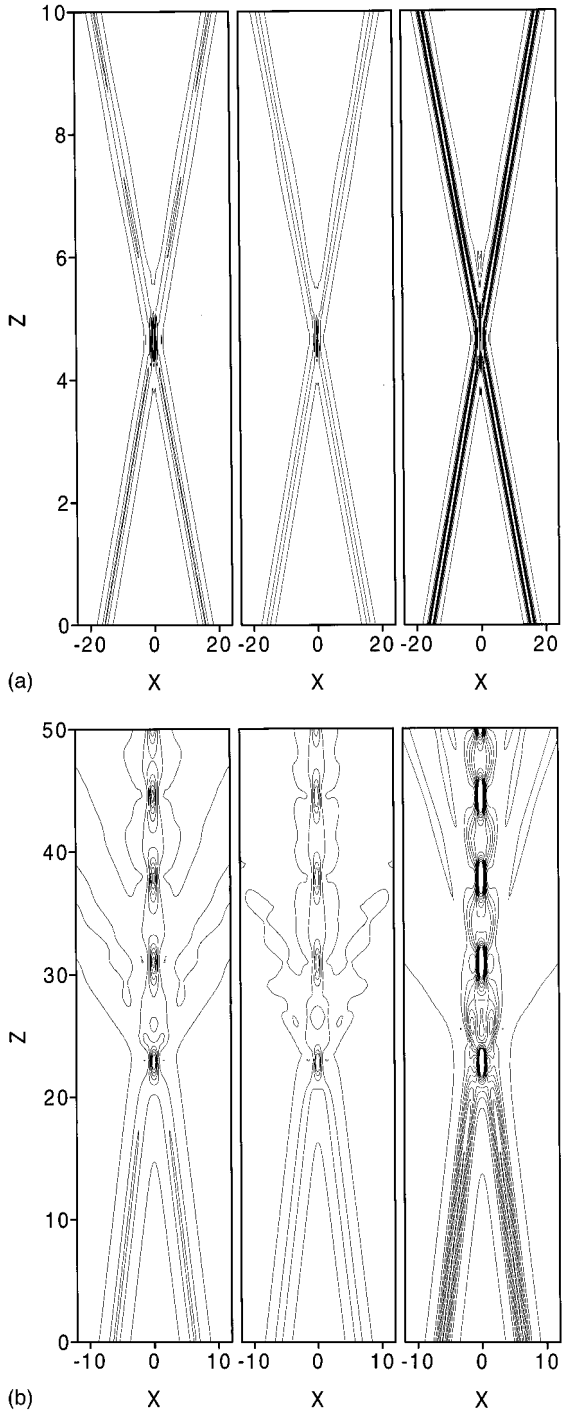


FIG. 3. Elastic (a) and inelastic (b) collisions of vectorial SWs. Parameters: $\alpha=1$, $\beta=0.8$; relative velocities $v=\delta X/\delta Z$: (a) $v=\pm 3$, (b) $v=\pm 0.2$.

turns out to be convenient to partially undo our previous transformations because the governing equations and the scaling should not depend on the parameters $\alpha$ and $\beta$ explicitly. Similar to [28], we rescale the fields as

$$\hat{A}_1=\gamma^2 A_1(\gamma X,\gamma^2 Z)\exp\left(i\frac{\beta}{\delta}Z\right),$$

$$\hat{A}_2=\gamma^2 A_2(\gamma X,\gamma^2 Z)\exp\left(i\frac{\delta}{\beta}Z\right), \tag{35}$$

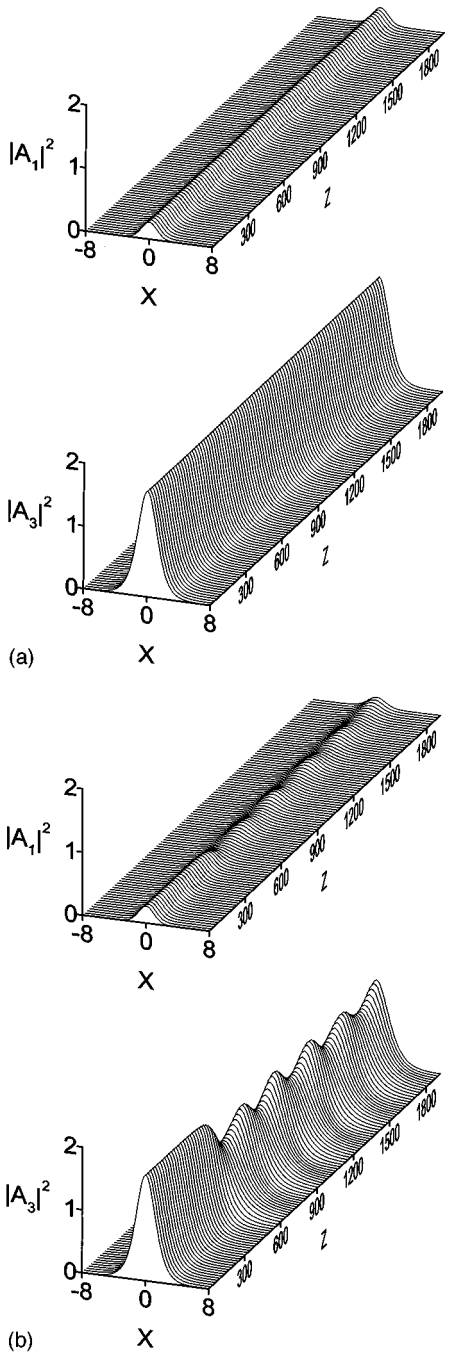


FIG. 4. Stable and unstable propagation of vectorial solitons. Parameters: (a) $\alpha=0.156$, $\beta=0.778$; (b) $\alpha=0.156$, $\beta=0.783$ ($\delta=1$, $\sigma=2$).

$$\hat{A}_3=\gamma^2 A_3(\gamma X,\gamma^2 Z)\exp\left(i\left[\frac{\beta}{\delta}+\frac{\delta}{\beta}\right]Z\right),$$

where the scaling parameter $\gamma$ has been introduced as

$$\gamma=\left(\frac{|q|}{\alpha-\sigma(\beta/\delta+\delta/\beta)}\right)^{1/2}.$$

Note that the transformation (35) also changes the conserved quantities to

$$\hat{Q}=\gamma^3 Q,\quad \hat{R}=\gamma^3 R,\quad \hat{H}=\gamma^5 H. \tag{36}$$

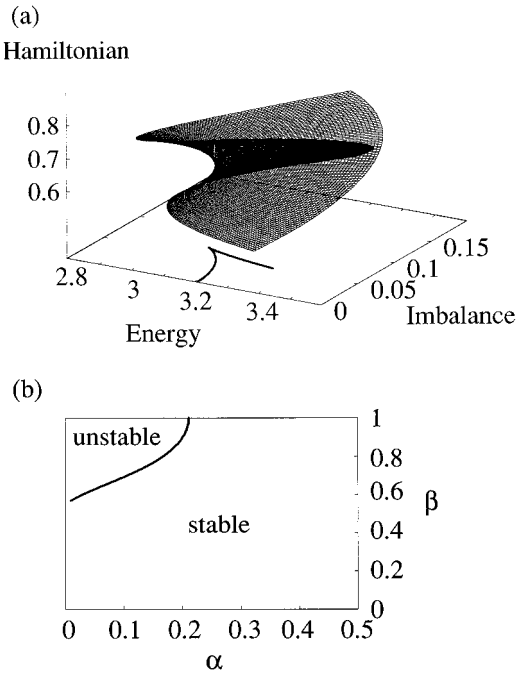


FIG. 5. Stability of vectorial SWs. (a) Hamiltonian vs energy $Q$ and energy imbalance $R$, the turning points of the surface are given at the bottom of the plot. (b) Critical line between the stable and unstable areas.

In Fig. 5(a) the Hamiltonian $\hat{H}$ is plotted as a function of the conserved quantities' energy $\hat{Q}$ and imbalance $\hat{R}$. Although the Hamiltonian is a unique function of the parameters $\alpha$ and $\beta$ this surface is multivalued. The critical line which separates stable from unstable domains is projected onto the $\alpha$-$\beta$ plane in Fig. 5(b). Thus the SWs become unstable if the vector function $(\hat{Q}(\alpha,\beta),\hat{Q}(\alpha,\beta))$ is not locally invertible or if the following expression holds:

$$\frac{\partial\hat{Q}}{\partial\alpha}\frac{\partial\hat{R}}{\partial\beta}-\frac{\partial\hat{Q}}{\partial\beta}\frac{\partial\hat{R}}{\partial\alpha}. \tag{37}$$

It is evident that our preliminary results are validated, viz., that the domain of instability is largest for the scalar case ($\beta=1$) and shrinks with increasing imbalance (decreasing $\beta$). To accomplish the limit $\alpha\to 0$ is not straightforward and needs particular care. This is because the width of the SWs tends to infinity in this limit. Rather than the critical numerical results we use the field shapes obtained by the variational approach to calculate the conserved quantities. This procedure results in a termination point $\beta_{\rm crit}$ for $\alpha\to 0$ with

$$\beta_{\rm crit}=\frac{\delta}{\sqrt{2}}(\sqrt{3}\pm 1). \tag{38}$$

We double checked the results concerning the stability of the SWs by numerical means (BPM calculations) and found a reasonable agreement.

The most surprising result of this stability analysis is the stabilizing effect of the energy imbalance. Already a very weak imbalance prevents the decay of the SWs. If we compare the results displayed in Figs. 2(b) and 5(b) we find that

in the spatial case no instability occurs if the relative energy imbalance $(R/Q)$ exceeds the very small value of 0.022.

## V. CONCLUSION

In this work, we have investigated solitary waves mediated by the vectorial or type-II interaction in a nonlinear optical medium in the presence of diffraction or dispersion. We derived the basic set of equations to describe the propagation of both spatial and temporal SWs. Some analytical expressions to estimate the peak amplitudes of the SWs were found. To determine the complete shape of the SWs under investigation a variational approach and direct numerical computations were used. An excellent agreement between both methods could be obtained. Studying the collision behavior of the SWs we found two SWs to fuse for small relative velocities as expected for a nonintegrable system we found. The new parameter $\beta$ or the energy imbalanced $R$ introduced by the vectorial model influences the stability of the solutions. Already a rather weak energy imbalance stabilizes the SWs. Unstable SWs are found in the vicinity of the scalar model (very small energy imbalance) only. They need not decay completely but may transform into long-living oscillating solutions.


[1] L. Allen and J. H. Eberly, *Optical Resonance and Two-Level Atoms* (Wiley, New York, 1975).

[2] J. S. Aitchison, A. M. Weiner, Y. Silberberg, M. K. Oliver, J. L. Jackel, D. E. Leaird, E. M. Vogel, and P. W. E. Smith, Opt. Lett. **15**, 471 (1990).

[3] J. S. Aitchison, K. Al-Hemiari, C. N. Ironside, R. S. Grant, and W. Sibbett, Electron. Lett. **28**, 1879 (1992).

[4] S. Maneuf, R. Desailly, and C. Froehly, Opt. Commun. **65**, 193 (1988).

[5] G. P. Agrawal, *Nonlinear Fiber Optics*, 2nd ed. (Academic, San Diego, 1995).

[6] A. Hasegawa, *Optical Solitons in Fibers* (Springer-Verlag, Berlin, 1990).

[7] R. DeSalvo, D. J. Hagan, M. Sheik-Bahae, G. I. Stegeman, E. W. Van Stryland, and H. Vanherzeele, Opt. Lett. **17**, 28 (1992).

[8] R. Schiek, M. L. Sundheimer, D. Y. Kim, Y. Baek, G. I. Stegeman, H. Seilbert, and W. Sohler, Opt. Lett. **19**, 1949 (1994).

[9] M. L. Sundheimer, Ch. Bossard, E. W. Van Stryland, G. I. Stegeman, and J. D. Bierlein, Opt. Lett. **17**, 1397 (1993).

[10] M. L. Sundheimer, A. Villeneuve, G. I. Stegeman, J. D. Bierlein, Electron. Lett. **18**, 1400 (1994).

[11] D. J. Hagan, Z. Wang, G. Stegeman, E. W. Van Stryland, M. Sheik-Bahae, and G. Assanto, Opt. Lett. **19**, 1305 (1994).

[12] R. Schiek, Y. Baek, G. Krijnen, G. I. Stegeman, I. Baumann, and W. Sohler, Opt. Lett. **21**, 940 (1996).

[13] Y. Baek, R. Schiek, and G. I. Stegeman, Opt. Lett. **20**, 2168 (1995).

[14] Y. N. Karamzin, and A. P. Sukhorukov, Pis'ma Zh. Éksp. Teor. Fiz. **20**, 734 (1974) [JETP Lett. **20**, 339 (1974)]; M. J. Werner and P. D. Drummond, J. Opt. Soc. Am. B **10**, 2390 (1993).

[15] K. Hayata and M. Koshiba, Phys. Rev. Lett. **71**, 3275 (1993).

[16] R. Schiek, J. Opt. Soc. Am. B **10**, 1848 (1993).

[17] C. R. Menyuk, R. Schiek, and L. Torner, J. Opt. Soc. Am. B **11**, 2434 (1994).

[18] L. Torner, Opt. Commun. **114**, 136 (1995).

[19] L. Torner, C. R. Menyuk, and G. Stegeman, J. Opt. Soc. Am. B **12**, 889 (1995).

[20] A. V. Buryak and Y. S. Kivshar, Phys. Lett. A **197**, 407 (1995).

[21] V. Steblina, Y. S. Kivshar, M. Lisak, and B. A. Malomed, Opt. Commun. **118**, 345 (1995).

[22] D. E. Prelinkovsky, A. V. Buryak, and Y. S. Kivshar, Phys. Rev. Lett. **75**, 591 (1995).

[23] L. Torner, D. Mihalache, D. Mazilu, and N. N. Akhmediev, Opt. Lett. **20**, 2183 (1995).

[24] C. Etrich, U. Peschel, B. Malomed, and F. Lederer, Phys. Rev. A **52**, R3444 (1995).

[25] D. M. Baboiu, G. I. Stegeman, and L. Torner, Opt. Lett. **20**, 2282 (1995).

[26] R. Schiek, Y. Baek, and G. I. Stegeman, Phys. Rev. E **53**, 1138 (1996).

[27] W. E. Torruellas, Z. Wang, D. J. Hagan, E. W. Van Stryland, and G. I. Stegeman, Phys. Rev. Lett. **74**, 5036 (1995).

[28] A. V. Buryak, Y. S. Kivshar, and V. V. Steblina, Phys. Rev. A **52**, 1670 (1995).

[29] J. A. Armstrong, N. Bloembergen, J. Ducuing, and P. S. Pershan, Phys. Rev. **127**, 1918 (1962).

[30] Y. R. Shen, *The Principles of Nonlinear Optics* (Wiley, New York, 1984), Chap. 6.5.

[31] S. Trillo and G. Assanto, Opt. Lett. **19**, 1825 (1994).

[32] A. L. Belostotsky, A. S. Leonov, and A. V. Meleshko, Opt. Lett. **19**, 856 (1994).

[33] G. Assanto, G. I. Stegeman, M. Sheik-Bahae, and E. Van Stryland, IEEE J. Quantum Electron. **QE-31**, 673 (1995).

[34] A. Kobyakov, U. Peschel, and F. Lederer, Opt. Commun. **124**, 184 (1996).

[35] A. Kobyakov and F. Lederer, Phys. Rev. A **54**, 3455 (1996).

[36] L. Lefort and A. Barthelemy, Electron. Lett. **31**, 910 (1995).

[37] G. Assanto, Z. Wang, D. J. Hagan, and E. W. Van Stryland, Appl. Phys. Lett. **67**, 2120 (1995).

[38] L. Lefort and A. Barthelemy, Opt. Lett. **20**, 1749 (1995).

[39] H. T. Tran, Opt. Commun. **118**, 581 (1995).

[40] E. A. Kuznetsov, A. M. Rubenchik, and V. E. Zakharov, Phys. Rep. **142**, 103 (1986); D. J. Mitchel and A. W. Snyder, J. Opt. Soc. Am. B **10**, 1572 (1993); L. Torner, D. Mihalache, D. Mazilu, and N. N. Akhmediev, Opt. Lett. **20**, 2183 (1995).